A Thioredoxin from the Hyperthermophilic Archaeon *Methanococcus jannaschii* Has a Glutaredoxin-like Fold but Thioredoxin-like Activities[†]

Duck Yeon Lee,[‡,§] Byung-Yoon Ahn,[§] and Key-Sun Kim*[,‡]

Structural Biology Center, Korea Institute of Science and Technology, P.O. Box 131, Cheongryang, Seoul, 130-650, Korea, and Graduate School of Biotechnology, Korea University, Seoul, 136-701, Korea

Received January 7, 2000; Revised Manuscript Received March 28, 2000

ABSTRACT: A thioredoxin homologue (Mj0307) from the hyperthermophilic archaeon *Methanococcus jannaschii* (*Mj*TRX) was cloned, produced in *E. coli*, and compared to the thioredoxin from *E. coli* (*E*TRX). The secondary structure profile of *Mj*TRX obtained by NMR spectroscopy shows that it has four β-sheets and three α-helices arranged in $\beta\alpha\beta\alpha\beta\beta\alpha$, similar to that of glutaredoxin. However, *Mj*TRX supports the growth of T7 bacteriophage in *E. coli* and is weakly reduced by the thioredoxin reductase from *E. coli*, indicating that *Mj*TRX is functionally closer to a thioredoxin than a glutaredoxin. *Mj*TRX has higher specific insulin reductase activity than *E*TRX and retained its full activity over 4 days at 95 °C, whereas *E*TRX lost its activity in 150 min. The standard state redox potential of *Mj*TRX is about −277 mV, which is the lowest value thus far known among redox potentials of the thioredoxin superfamily. This indicates that the lower redox potential is necessary in keeping catalytic disulfide bonds reduced in the cytoplasm and in coping with oxidative stress in an anaerobic hyperthermophile.

Thioredoxins are small acidic proteins containing two redox-active half-cystine residues in an exposed active site with the sequence Cys-X-X-Cys (X corresponds to any amino acid) that function as protein disulfide reductases in numerous biological reactions. Thioredoxin was initially isolated in vitro as a hydrogen donor for ribonucleotide reductase (*1*). Oxidized thioredoxin is reduced by thioredoxin reductase with NADPH as a hydrogen donor (*2, 3*). *Escherichia coli* thioredoxin (*E*TRX) also plays a key role in promoting egress and assembly of the filamentous phages f1 (*4*) and M13 (*5*, *6*). It also participates in the DNA replication of bacteriophage T7 as a component of the phage-encoded DNA polymerase complex. An active T7 DNA polymerase complex is composed of T7 DNA polymerase (gene 5 protein) and *E*TRX in a one-to-one stoichiometry (*7*−*10*) and has some 1000-fold higher processivity of polymerization than T7 DNA polymerase alone (*11*). Glutaredoxin has been identified and characterized in *E. coli* mutants lacking thioredoxin but with fully active NADPH-dependent deoxyribonucleotide synthesis (*12*). It catalyzes glutathione (GSH) disulfide transhydrogenase reactions and is specific for a monothiol glutathione. In a thioredoxin/glutaredoxin double mutant of *E. coli*, glutaredoxin-3 is a hydrogen donor for ribonucleotide reductase (*13*). The thioredoxin fold containing an active site Cys-X-X-Cys motif is found not only in thioredoxin and glutaredoxin but also in DsbA and DsbC in the periplasm of Gram-negative bacteria, which are involved in catalyzing disulfide formation during the folding of exported proteins (*14*, *15*), and in the eukaryotic protein disulfide isomerase (PDI) (*16*). Although these thioredoxin-like proteins have similar active-site sequences, they have different redox functions. Thioredoxin/glutaredoxin systems also play a critical role in redox homeostasis in the cytosol and elimination of harmful oxidants. When *E. coli* is exposed to reactive oxygen species (ROS) such as $O_2^{-\bullet}$ and hydrogen peroxide, the transcription factor OxyR and chaperone Hsp33 are activated. The activated OxyR not only triggers the expression of enzymes that remove the oxidant, but also increases the expression of disulfide reductants, which restores the overall reducing conditions of the cell and deactivates OxyR and Hsp33 by reducing disulfide bonds (*17*−*21*).

Recently, the whole genome sequences of the hyperthermophilic archaea *Methanococcus jannaschii* (*22*), *Methanobacterium thermoautotrophicum* (*23*), *Pyrococcus horikoshii* (*24*), *Archaeoglobus fulgidus* (*25*), and *Aeropyrum pernix* (*26*) and the hyperthermophilic bacteria *Aquifex aeolicus* (*27*) and *Thermatoga maritime* (*28*) have been determined. These hyperthermophiles also have proteins with thioredoxin/glutaredoxin motifs suggesting the ubiquity of this system in nature. Hyperthermophiles are generally capable of growing under extreme conditions such as low pH, high pressure, and high salt concentration. Most of these organisms are anaerobes, have extraordinarily heat-stable proteins, and use ingenious strategies for stabilizing nucleic acids and other macromolecules in vivo (*29*). In *M. jannaschii*, a thioredoxin-like protein (*Mj*TRX) with a Cys-Pro-His-Cys in the active site (annotated as thioredoxin; MJ0307) and a thioredoxin reductase homologue (MJ1536) were identified (*22*). *Mj*TRX is 85 amino acids long, similar to glutaredoxin in size, but has Cys-Pro-His-Cys in the active site that is different from either thioredoxin or glutaredoxin

[†] This work was supported in part by a grant from Critical Technology 21 of the Ministry of Science and Technology in Korea and by KIST2000 Program to K.-S.K.

* Corresponding author. Tel: (+82-2) 958-5934; Fax: (+82-2) 958-5939; E-mail: keysun@kist.re.kr.

[‡] Korea Institute of Science and Technology.

[§] Korea University.

10.1021/bi000035b CCC: $19.00
Published on Web 05/09/2000

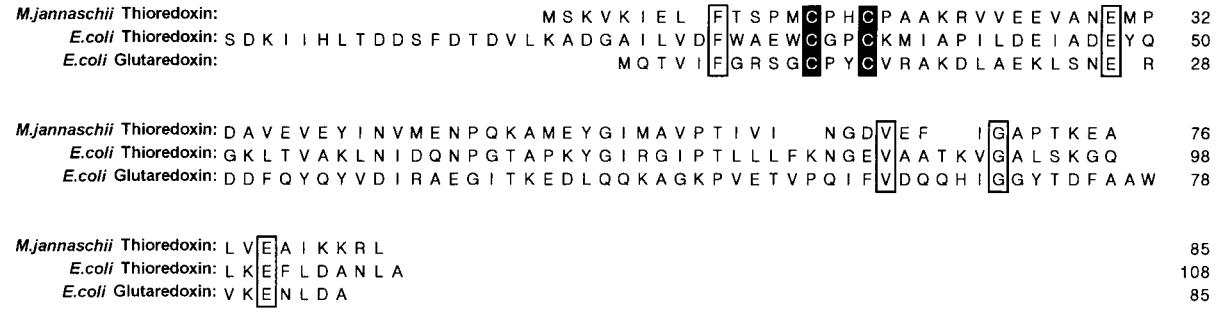

FIGURE 1: Sequence alignment of some thioredoxin family proteins. Conserved amino acids are in white boxes, and active-site cysteines are in black boxes.

(Figure 1). We characterized MJ0307 protein (*Mj*TRX) from *M. jannaschii* and compared it to thioredoxin from *E. coli* to understand the possible role of thioredoxin in hyperthermophilic archaebacteria, considered to be the most ancient of all living organisms (*30, 31*). We show that *Mj*TRX from *M. jannaschii* exhibits biochemical activities similar to thioredoxin although the structure of it is more like glutaredoxin. We also show that *Mj*TRX is the most reductive thioredoxin among known thioredoxin-like proteins.

EXPERIMENTAL PROCEDURES

Genomic DNA from M. jannaschii. M. jannaschii (DSM 2661) were obtained from Deutsche Sammlung von Mikroorganism (DSM, Germany) and grown at 85 °C, pH 6.5. Culture media and genomic DNAs of these strains were prepared by the modified method of Guagliardi et al. (*31*).

Protein Expression and Purification. The complete coding sequence of thioredoxin was amplified by 30 cycles of polymerase chain reaction (PCR) (denaturing at 96 °C, annealing at 58 °C, and extension at 72 °C) using genomic DNA as a template. The PCR fragments of *Mj*TRX were digested with *Nde*I and *Bam*HI and cloned into an expression vector, pET15b (Novagen). *E. coli* BL21(DE3) harboring each recombinant plasmid was grown at 37 °C until $A_{600} \cong 1$, and the recombinant proteins were induced with 0.4 mM isopropyl-1-thio-β-D-galactopyranoside for 2 h. Cell paste obtained by centrifugation at 5000 rpm for 15 min was resuspended in a lysis buffer (50 mM potassium phosphate, pH 8.0, and 300 mM KCl) and disrupted by ultrasonication. DNase I (10 μg/mL) and RNase (10 μg/mL) were added to the cell extract and incubated for 30 min at room temperature to remove nucleic acid. The crude extract was heated at 85 °C for 30 min, and centrifuged at 16 000 rpm for 20 min. The supernatant was loaded onto a nickel nitrilotriacetic acid−agarose resin (Ni-NTA) column (Qiagen) and eluted with an elution buffer (50 mM potassium phosphate, pH 6.0, 300 mM KCl, and 10% glycerol) containing 0.3 M imidazole. The polyhistidine tag was removed by thrombin for 12 h at room temperature. The cleaved protein solution was dialyzed and loaded onto a DEAE-Sepharose column equilibrated with dialysis buffer (50 mM potassium phosphate, pH 6.5, and 2 mM EDTA). The flow-through was concentrated by ultrafiltration using an Amicon ultrafiltration apparatus (Amicon). The concentrated sample was further purified by gel filtration chromatography using a Superdex G75 column (Pharmacia, 1 cm × 30 cm) in 50 mM potassium phosphate (pH 6.5), 2 mM EDTA, and 300 mM KCl. Each purified protein was confirmed with N-terminal amino acid sequencing. *E*TRX was expressed and purified as described by Langsetmo et al. (*32*) with anion exchange and gel filtration chromatography. The uniform isotope labeling of ^{13}C, ^{15}N atoms in *Mj*TRX was achieved by growing cells in M9 minimal medium with 1.0 g of $^{15}NH_4Cl$/L and 2.0 g of [^{15}C]glucose/L. NMR samples were prepared by dissolving about 10 mg of protein in 0.5 mL of either 90% H_2O/10% ^2H_2O or 99.9% ^2H_2O. The pH was adjusted to 3.30 ± 0.05 (glass electrode, uncorrected) with concentrated NaO^2H.

Thioredoxin/Glutaredoxin Activity Assay and Thermal Stability. The *Mj*TRX activity was routinely determined with the insulin precipitation assay described by Holmgren (*33*). The standard assay mixture contained 0.1 M potassium phosphate (pH 7.0), 2 mM EDTA, 0.13 mM bovine insulin, and 2 μM *Mj*TRX, and the reaction was initiated upon the addition of 1 mM dithiothreitol. An increase of the absorbance at 650 nm was monitored at 30 °C. The DTNB-coupled reduction of thioredoxin with thioredoxin reductase of *E. coli* was also used to determine thioredoxin activity (*34*). The activity of thioredoxin reductase was assayed at 30 °C by measuring the absorbance increase at 412 nm at various concentrations of *Mj*TRX (2.2, 4.4, 9, and 12 μM) in a reaction buffer [2 mM DTNB, 0.24 mM NADPH, and 0.5 unit of *E. coli* thioredoxin reductase in 1.0 mL of 100 mM Tris-HCl (pH 8.0)]. As a positive control, 2 μM *E*TRX was used, and the reaction was started by adding thioredoxin reductase in a reaction mixture. Glutaredoxin activity was measured using the glutathione-disulfide transhydrogenase assay described by Gan et al. (*35*). The standard assay mixture consisted of 100 mM potassium phosphate (pH 8.0), 1 mM EDTA, 1 mM GSH, 2.5 mM L-cystine, 0.2 unit of glutathione reductase, 0.3 mM NADPH, and 2 μM *Mj*TRX. The enzyme activity was monitored at 30 °C by the absorbance at 340 nm. The thioredoxin concentrations of *E. coli* and *M. jannaschii* were determined using molar extinction coefficients of 13 700 M^{-1} cm^{-1} (*34*) and 3105 M^{-1} cm^{-1} (*36*) at 280 nm, respectively. To evaluate the thermal stability of thioredoxins, *Mj*TRX and *E*TRX were incubated at 95 °C, and the residual insulin reductase activity of thioredoxins was measured at 30 °C as described above. All reaction tubes were screw-capped to prevent the evaporation of solution during the incubation at 95 °C.

Determination of the pK_a Values of Thiol Groups. The thiolate ion has a higher absorption at 240 nm with an ϵ_{240} of about 4000 M^{-1} cm^{-1} than the un-ionized thiol group (*37*−*39*). Therefore, the pK_a values of thiol groups can be determined by monitoring UV absorption during pH titration. The pH of *Mj*TRX solution (0.1 mM) was adjusted by NaOH

or HCl from 3 to 8.5 and the measured UV absorption at 240 nm, and the protein concentration was determined by absorption at 280 nm. To measure thiolate-dependent absorption only at 240 nm, absorption of either oxidized thioredoxin or reduced and akylated thioredoxin by iodoacetamide was subtracted. The UV absorption of oxidized thioredoxin or alkylated thioredoxin at 240 nm was negligible the whole pH range. The pH-dependent absorption was fitted according to the Henderson−Hasselbach equation to obtain the pK_a value of thiol.

Interaction between T7 DNA Polymerase and MjTRX. An expression vector harboring *Mj*TRX was introduced into the TRX-defective *E. coli* strain (BH2012), and the protein was induced with 0.4 mM IPTG for 40 min. The cell with the expressed protein was used as plating bacteria and was infected with T7 phage as described by Huber et al. (*40*). The plasmid (pCJF4) encoding *E. coli* thioredoxin, thioredoxin-defective *E. coli* strains, *E. coli* thioredoxin reductase, and T7 phage were a generous gift from Prof. C. J. Lim (Kangwon National University, Korea).

NMR Spectroscopy. The heteronuclear NMR experiments were carried out with a ^{15}N-labeled or a ^{13}C-,^{15}N-labeled sample in 90% H_2O/10% ^2H_2O. All experiments were done using a Varian UNITY*plus* 600 spectrometer (at Advance Analysis Center of KIST) at 30 °C. The concentration of protein was about 2 mM. Two-dimensional ^{1}H−^{13}C constant time HSQC,[1] 3D ^{1}H−^{15}N NOESY-HSQC, ^{1}H−^{15}N TOCSY-HSQC (*41*), HNHA (*42*), HCACO (*43*), and HNCO (*44*) were acquired with the ^{13}C- or ^{15}N-labeled sample, and ^{13}C-, ^{15}N-edited NOESY (*45*), HNCACB, and CBCA(CO)NH (*46*) were acquired with the ^{13}C-, ^{15}N-labeled sample. NMR data were processed using the program NMRPipe (*47*). Starting with the identifications of ^{15}N and HN chemical shifts in ^{1}H−^{15}N HSQC, spin systems were partially identified in ^{1}H−^{15}N TOCSY-HSQC, and the sequential assignments of each amino acid were made using HNCACB, CBCA(CO)NH, and ^{1}H−^{15}N NOESY-HSQC with mixing time of 120 ms. Chemical shift indices were calculated by the method of Wishart et al. (*48*).

Redox Potential of MjTRX. For the determination of the redox potential of *Mj*TRX, we used the modified method of Åslund et al. (*49*). The *Mj*TRX−*E*TRX redox equilibrium reactions (100 μL) contained 50 μM of each protein in a degassed and N_2-purged solution of 100 mM potassium phosphate (pH 7.0) and 1 mM EDTA. The reduced form of *Mj*TRX was prepared immediately before use by incubation of protein for 2 h at room temperature with 10 mM dithiothreitol, followed by HPLC gel filtration chromatography (TSK-Gel-G2000 SWXL, 7.8 mm i.d. × 30 cm long). Redox reactions were initiated by adding the reduced form of *Mj*TRX to the oxidized form of *E*TRX, and then the sample was left to equilibrate at room temperature. After 4, 9, and 12 h, an aliquot (20 μL) of each sample was quenched by adding 10 μL of 1.0 M phosphoric acid to a final pH of 2.5 and analyzed by a reverse-phase HPLC. The reduced and oxidized forms of the proteins present in the samples were separated by reverse-phase HPLC on a VyDAC C_{18} column and quantitated. The mechanism of thiol−disulfide exchange is believed to be a two-step reaction proceeding through a mixed disulfide intermediate. The breakdown of the protein−protein mixed disulfide appears to be very rapid, as it is not normally populated under standard conditions (*49*):

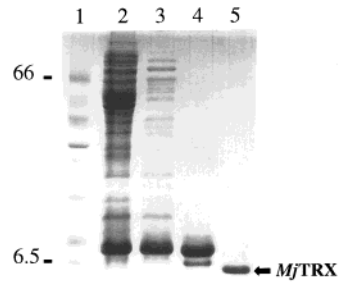

FIGURE 2: SDS−polyacrylamide gel electrophoresis analysis of proteins of each purification step. A sample of each purification step was analyzed by SDS−polyacrylamide gel electrophoresis (15%) and stained with Coomassie blue. Lane 1, molecular weight markers (Sigma, low range); lane 2, crude cell extract; lane 3, soluble supernatant after heat treatment (85 °C for 30 min); lane 4, eluted *Mj*TRX with imidazole buffer from Ni-NTA resin; lane 5, *Mj*TRX after removing polyhistidine tag and purified by Superdex G75 gel filtration chromatography.

$$A-SH_2 + B-S_2 \overset{K_1}{\rightleftarrows} HSAS-SBSH \overset{K_2}{\rightleftarrows} A-S_2 + B-SH_2 \quad (1)$$

$$K_1K_2 = K_{12} = [A-S_2][B-SH_2]/[A-SH_2][B-S_2] \quad (2)$$

$$E^o_A - E^o_B = \Delta E^o_{AB} = (RT/nF) \ln K_{12} \quad (3)$$

where A is *Mj*TRX and B is *E*TRX. The difference in redox potential between the two proteins, ΔE^o_{AB}, can then be obtained using the Nernst equation (eq 3), where n is the number of electrons transferred in the reaction (here $n = 2$), F is Faraday's constant (23,040.612 cal·mol^{-1}·V^{-1}), and R is the gas constant (1.987 cal·K^{-1}·mol^{-1}).

RESULTS

Preparation of MjTRX. As the optimal growth temperature of *M. jannaschii* is about 85 °C, proteins from this organism are expected to be stable at 85 °C. In purifying the hyperthermophile proteins expressed in *E. coli*, heat treatment is highly beneficial. *Mj*TRX was obtained in about 70% pure form as most other *E. coli* proteins were denatured by heat treatment. The further purification of *Mj*TRX was achieved by Ni-NTA agarose column and gel filtration chromatography. The final yield of *Mj*TRX after proteolytic removal of the polyhistidine tag was about 10 mg per liter of culture (Figure 2) with purity higher than 95%. The purified *Mj*TRX has three extra amino acid residues (Gly-Ser-His) at its N-terminus. The yield of *E*TRX purified as described in Langsetmo et al. (*32*) was about 20 mg per liter of culture.

Thioredoxin/Glutaredoxin Activity Assay. When the specific activity of each protein was compared at 30 °C and pH 7.0 by the insulin reduction assay, *Mj*TRX showed molar specific activity higher than that of *E*TRX (Figure 3A) in about 1.4 times. And *Mj*TRX retained its full activity over 4 days at 95 °C whereas *E*TRX lost its activity completely in 150 min (Figure 3B). The insulin reductase activity is dependent on the ionic status of active-site thiols. Therefore, we determined the pK_a values of thiol groups. The ϵ_{240} was

[1] Abbreviations: NOESY, nuclear Overhauser effect enhancement spectroscopy; HSQC, heteronuclear single-quantum coherence; TOCSY, total correlation spectroscopy.

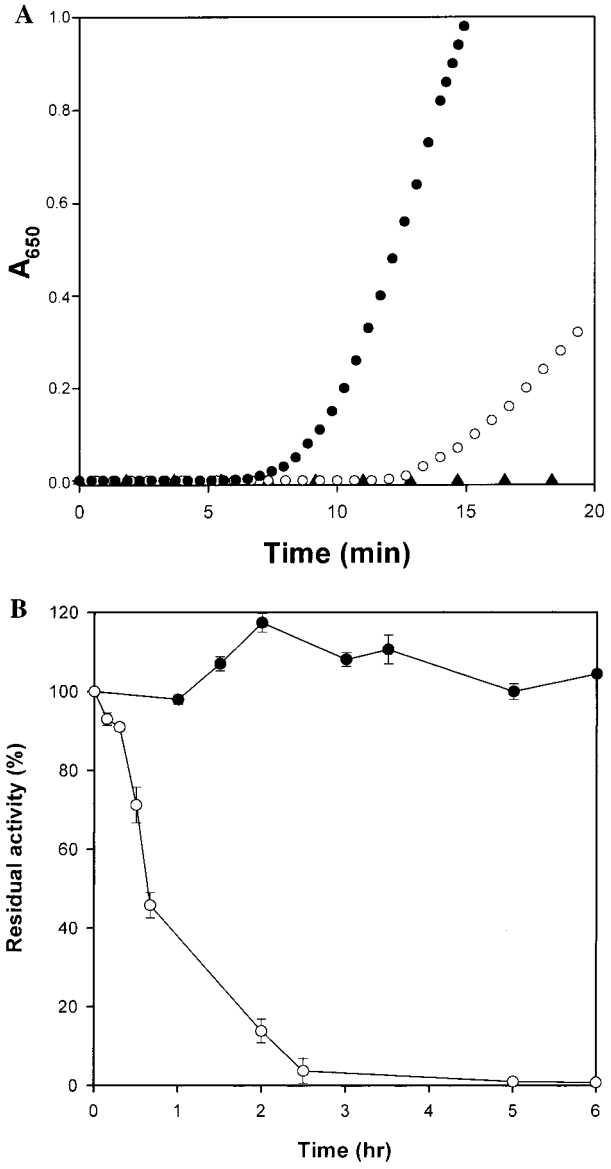

FIGURE 3: Reduction of insulin disulfides and thermal stability of *Mj*TRX and *E*TRX. (A) The activity assay was performed as described in the text. Purified *Mj*TRX (●) and *E*TRX (○) (2 μM each) were added to the reaction mixture, and the amount of reduced insulin was monitored by the absorption at 650 nm. Reaction mixture without thioredoxin was used as a negative control (▲). The activities for *Mj*TRX and *E*TRX calculated from the figure were 0.14 and 0.10 ΔA_{650}/min, respectively. (B) Residual insulin reductase activities of *Mj*TRX (●) and *E*TRX (○) were measured with the incubation time. All samples were incubated at 95 °C.

increased by about 8000 by titration, indicating that two thiol groups were involved in titration, but a single pK_a value was enough to fit data to the Henderson−Hasselbach equation (Figure 4). The pK_a values of both thiols are 6.28 ± 0.07. Thioredoxin reduces other proteins and is reduced in turn by an NADPH-dependent thioredoxin reductase in *E. coli*. We tested whether *Mj*TRX is reduced by *E*TRX reductase. As shown in Figure 5A, *E*TRX reductase could reduce *Mj*TRX. However, the recombinant *Mj*TRX reductase (*Mj*1356) could not reduce either *Mj*TRX or *E*TRX with NADPH as a hydrogen donor (data not shown), indicating that the *Mj*TRX system might not use NAD(P)H as a hydrogen donor and/or that another factor is involved in the thioredoxin system in *M. jannaschii*. We also tested whether

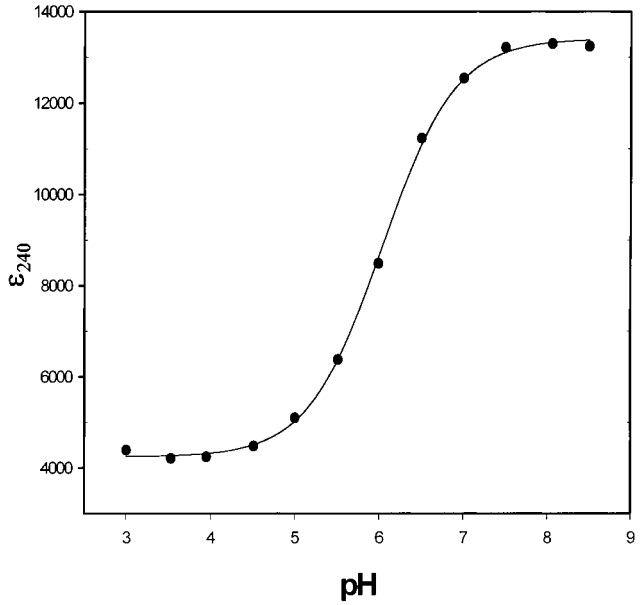

FIGURE 4: pK_a values of active-site thiols. The pK_a values of thiol groups are obtained by measuring the amount of thiolate concentration with pH. The data were fitted according to the Henderson−Hasselbach to obtain pK_a values.

*Mj*TRX has thiol-transferase activity by a glutathione-disulfide oxidoreductase. As indicated in Figure 5B, *Mj*TRX did not have a thiol-transferase activity.

Interaction between T7 DNA Polymerase and MjTRX. E. coli thioredoxin interacts with T7 DNA polymerase and improves the processivity of T7 DNA polymerase complex about 1000-fold, so the T7 bacteriophage cannot survive in a thioredoxin-deficient *E. coli* strain without complementation with thioredoxin (*50*). To test whether *Mj*TRX can complement the thioredoxin deficiency, the F^- thioredoxin-deficient mutant (BH2012) harboring a plasmid encoding *Mj*TRX was infected with T7 bacteriophage. After 12 h, the number of plaques formed by T7 bacteriophage was examined. About 400 phage plaques were seen on the wild-type *E. coli* lawn while about 250 were forming on the thioredoxin-deficient *E. coli* BH2012 lawn with *Mj*TRX complemented. The size of the plaques formed on the thioredoxin-deficient *E. coli* BH2012 lawn was smaller compared to plaques formed on the wild-type *E. coli* lawn. No plaques were seen on the thioredoxin-deficient *E. coli* BH2012 lawn without any thoredoxins expressed.

Secondary Structure of MjTRX. The chemical shifts of $^1H\alpha$, $^{13}C\alpha$, and carbonyl-^{13}C are affected by the secondary structures of protein. The resonances of $^1H\alpha$ in the helical conformation are shifted upfield, and those of $^{13}C\alpha$ and carbonyl-^{13}C in the same conformation are shifted downfield. On the other hand, the trend is reversed in the sheet conformation (*48*). In the helical conformation, $^3J_{HNH\alpha}$-coupling constants are lower than 5.5 Hz and NOEs of αN (i, i+3) are observed. In the sheet conformation, $^3J_{HNH\alpha}$-coupling constants become higher than 8 Hz (*51*). So the secondary structure of proteins can be estimated by NMR spectroscopy with high accuracy without calculating the three-dimensional structure. The chemical shift indices, $^3J_{HNH\alpha}$-coupling constants, and NOE connectivity (Figure 6) indicated that *Mj*TRX consists of three α-helices and four β-sheets arranged as $\beta\alpha\beta\alpha\beta\beta\alpha$, similar to glutaredoxin. It retains the so-called 'thioredoxin fold' but lacks the N-

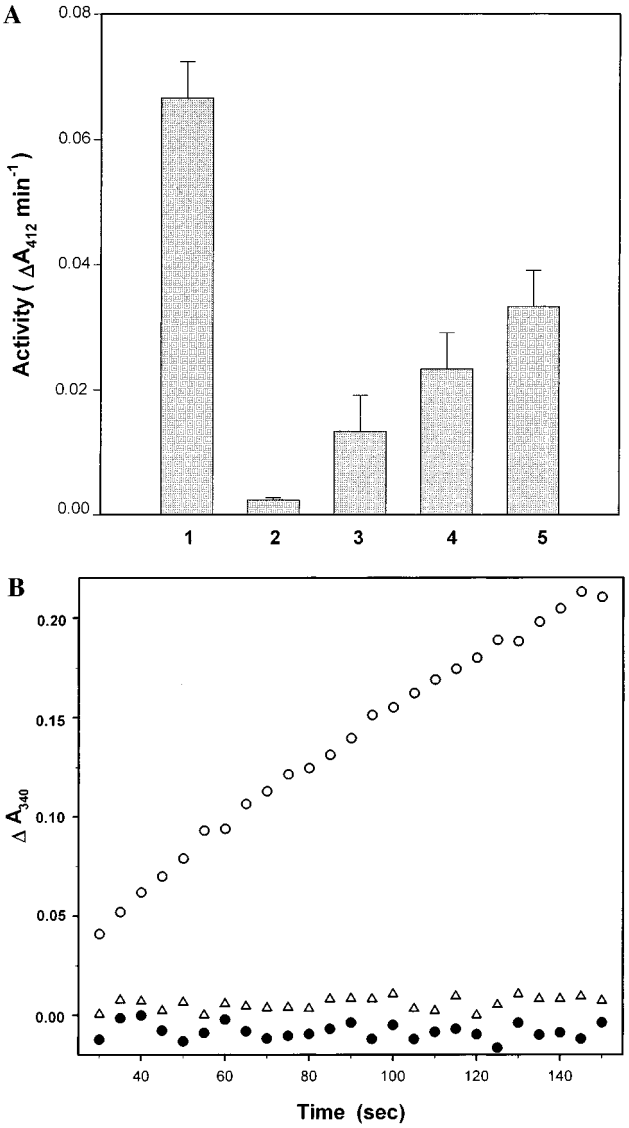

FIGURE 5: Reduction of *Mj*TRX by *E*TRX reductase and thiol-transferase activity of *Mj*TRX. (A) DTNB-coupled reduction of *Mj*TRX by *E*TRX reductase was monitored by the absorption at 412 nm at various concentrations of *Mj*TRX [1: *E*TRX (2 μM); 2−5: *Mj*TRX (2, 2.2 μM; 3, 4.4 μM; 4, 9 μM; 5, 12 μM)]. (B) Thiol-transferase activity was measured as described in the text. BSA was used as the negative control. Glutaredoxins from *E. coli* (○), *Mj*TRX (●), and BSA (Δ) are compared.

terminal β-sheet and α-helix of *E. coli* thioredoxin. *E*TRX has four α-helices and five β-sheets arranged as $\beta\alpha\beta\alpha\beta\alpha\beta\beta\alpha$.

Redox Potential of MjTRX. The difference of redox potential governs the reaction direction of two redox-active proteins, so the redox potential of proteins can be determined by direct protein−protein equilibration (*49*). In principle, differences in redox potential between two proteins, ΔE^{o}_{AB}, could be determined by the concentrations of their oxidized and reduced forms (eqs 1−3) at equilibrium. As shown in Figure 7, HPLC analysis of the reaction products showed that *E*TRX_ox decreased with time, while *E*TRX_red increased with incubation time (Figure 7B). *Mj*TRX_ox and *Mj*TRX_red coelute in the HPLC chromatogram (Figure 7A), but an equilibrium constant was calculated based on the reaction stoichiometry. When *Mj*TRX_red and *E*TRX_ox are mixed, *E*TRX_ox is reduced with the same molar equivalent of *Mj*TRX_red oxidized. So once we know the molar quantity of newly generated *E*TRX_red, the equilibrium constant can be calculated. Equilibrium between *Mj*TRX and *E*TRX was reached after 7 h, and the equilibrium constant (K_{12}) between them was $(0.584 \pm 6.5) \times 10^{-3}$ at pH 7.0. Thus, according to eq 3, *Mj*TRX has lower redox potential than *E*TRX by 6.95 ± 0.14 mV. The value of E^{o}_{ETRX} is −270 mV (*2*, *49*), so E^{o}_{MjTRX} is about −277 mV. When *Mj*TRX_ox and *E*TRX_red were mixed, *E*TRX_red could not reduce *Mj*TRX_ox, indicating that *Mj*TRX has lower redox potential compared to *E*TRX (Figure 7C). The redox potential of *Mj*TRX is the lowest redox potential among the known thioredoxin family proteins (Figure 7D).

DISCUSSION

Structure of MjTRX and Interaction with Virus Machinery. Bacteriophage T7 is able to form plaques on an *E. coli* $TrxA^{+}$ strain. The T7 DNA polymerase (gene 5 protein) is bound to the thioredoxin of the host to produce an active T7 polymerase complex. However, not all thioredoxins interact with T7 DNA polymerase. The glutaredoxin from *E. coli* (*2*) or thioredoxin from *Anabaena* (*52*) does not support T7 phage growth, whereas the thioredoxins from *Thiobacillus ferroxidans* (*53*), *Corynebacterium nephridii* (*54*), *and Rhodobactor sphaeroides* (*55*) are known to support T7 phase growth. *Mj*TRX is structurally similar to glutaredoxin (Figure 6), but *Mj*TRX does support the growth of T7 phage. In the active complex of T7 DNA polymerase with *E. coli* thioredoxin, the extended loop between helices H and H1 of T7 DNA polymerase wraps around *E. coli* thioredoxin and buries the active-site cysteines as well as Arg71-Gly72-Ile75-Pro76 (*56*). Complementation of *E*TRX by *Mj*TRX in T7 phage-infected, TRX-deficient *E. coli* strain shows that *Mj*TRX has the thioredoxin fold intact and the N-terminus of *E*TRX does not play a key role in T7 DNA polymerase complex formation. Furthermore, the substitution of either Cys14 or Cys17 by Ser still supported T7 phase growth, which was also observed in the case of *E*TRX (*40*, *57*). This result indicates that a serine substitution mutant is similar to the reduced wild-type protein in structure, and thiol groups are not required for T7 polymerase interaction as confirmed in *E*TRX. However, the amino acid residues of *Mj*TRX in the interacting region are different from those of *E*TRX, indicating that the flexibility of the extended loop in T7 DNA polymerase may play a role in structural adjustment for the better fit with *Mj*TRX. *Mj*TRX is more like glutaredoxin in structure, but reduction by *E. coli* thioredoxin reductase and its interactions with T7 polymerase indicate that it is closely related to thioredoxin in function. It may also have additional unknown functions that require a glutaredoxin-like structure. T4 glutaredoxin also reacts with *E. coli* thioredoxin reductase, but it fails to react with T7 polymerase (*2*). *Mj*TRX is much more stable than *E*TRX against heat inactivation, but the reason for this is not clear yet. Presently we are investigating factors contributing to protein stability using site-directed mutagenesis.

*Biochemical Activities. Mj*TRX is a member of the family of protein disulfide oxidoreductases. The sequence of its active center, Cys-Pro-His-Cys, is the same as that of *E. coli* DsbA, the most oxidizing member of the thiol/disulfide oxidoreductase family (*58*). The dipeptide located between the two active-site cysteines plays a critical role in determining the redox potential as well as the pK_a of the active-site

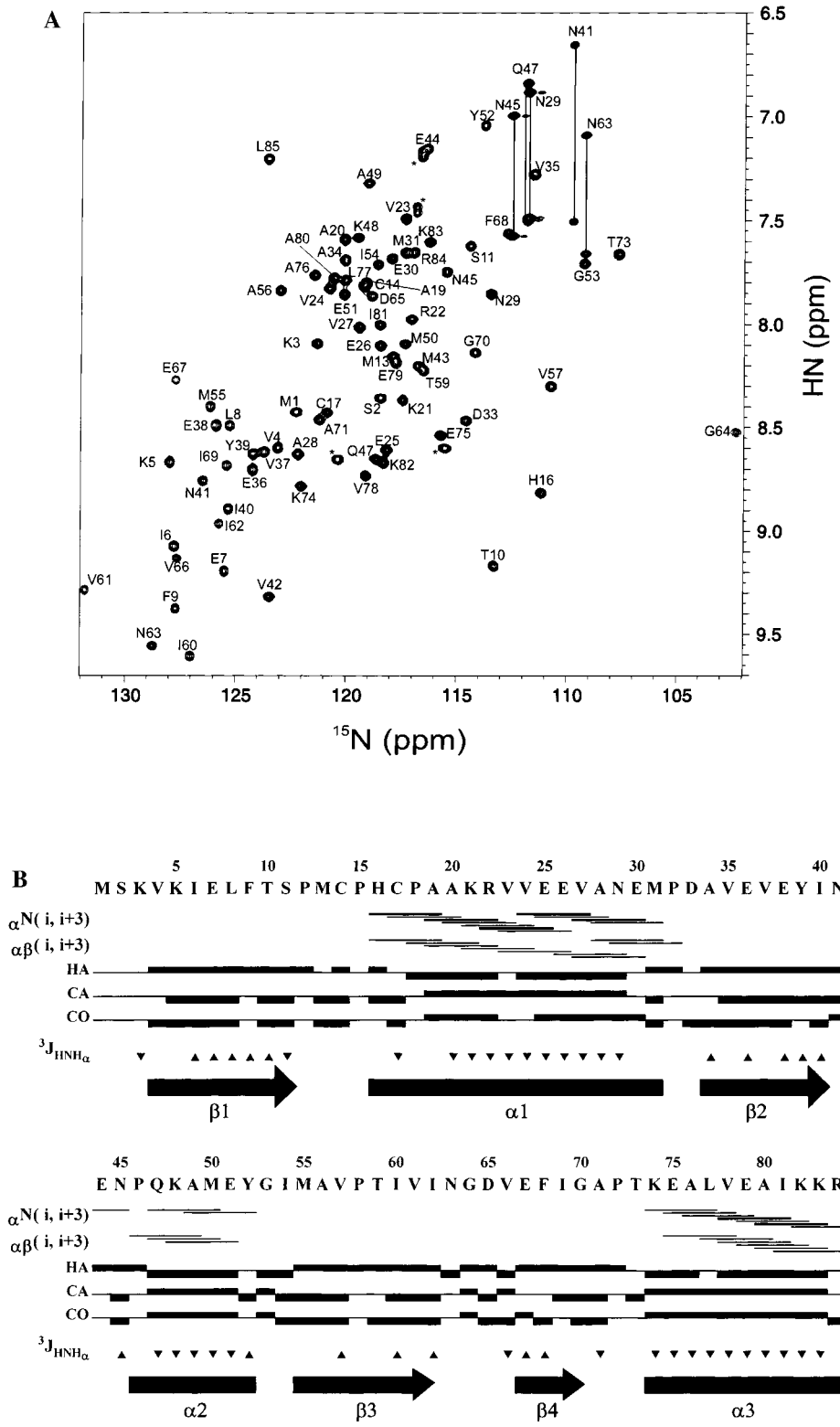

FIGURE 6: Summary of NOE connectivity, $^3J_{HNH\alpha}$ coupling constants, and chemical shift index. (A) $^1H-^{15}N$ HSQC spectrum of *Mj*TRX. The cross-peaks from the side chains of Asn and Gln are labeled with connecting lines. (*) Spurious peaks from the cloning artifact. (B) Secondary structures are assigned based on the NOE connectivity, $^3J_{HNH\alpha}$ coupling constants, and chemical shift index (*48*). The $^3J_{HNH\alpha}$ coupling constants smaller than 5.5 Hz (▼) and bigger than 8.0 Hz (▲) are shown.

thiols of oxidoreductases within the thioredoxin superfamily (*50*, *59*). Each subfamily possesses a characteristic dipeptide within the active site: Gly-Pro for thioredoxin, Pro-Thr for glutaredoxin, Pro-His for DsbA, and Gly-His for the eukaryotic protein disulfide isomerase. The redox potential of *Mj*TRX is −277 mV, but it has the same dipeptide as in DsbA, which has a redox potential of −125 mV. This indicates that amino acids outside of the active site are also important in determining redox potential (*60*). According to the mechanism of thioredoxin-catalyzed protein disulfide reduction of *E*TRX proposed by Holmgren (*61*), nucleophilic attack by the thiolate of Cys32 results in the formation of a transient mixed disulfide, which is followed by nucleophilic attack of the deprotonated Cys35 generating oxidized thiore-

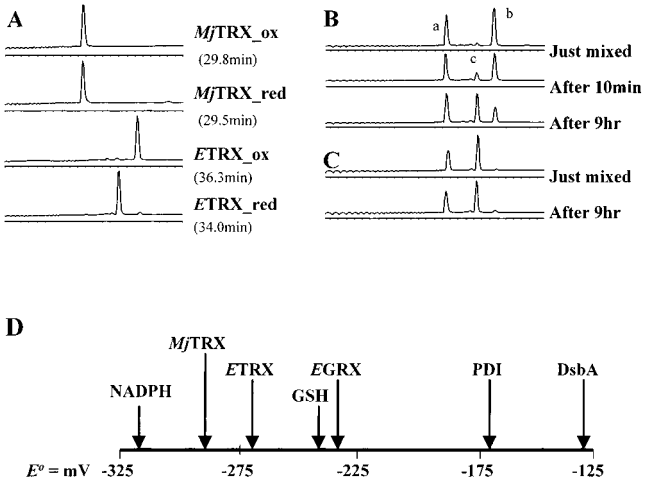

FIGURE 7: Redox potential measurement of *Mj*TRX and *E*TRX. *Mj*TRX_red and *E*TRX_ox were incubated for 4, 9, and 12 h at room temperature at a concentration of 50 mM each in 100 mM potassium phosphate, pH 7.0, followed by acid quenching to pH 2.5 before HPLC analysis. (A) Elution profiles of *E*TRX_ox, *E*TRX_red, *Mj*TRX_ox, and *Mj*TRX_red. (B) Equilibrium between *Mj*TRX_red and *E*TRX_ox. Decrease of *E*TRX_ox and growth of *E*TRX_red could be observed with time. *Mj*TRX_ox and *Mj*TRX_red elute very closely in the chromatogram, so the intensity of *Mj*TRX_red appears to be constant with time. (C) Equilibrium between *Mj*TRX_ox and *E*TRX_red. Even after 9 h, *E*TRX_ox could not be observed, indicating that *E*TRX cannot reduce *Mj*TRX. (D) Standard state redox potentials of the thioredoxin family of thiol-disulfide oxidoreductase. a, *Mj*TRX_red and *Mj*TRX_ox; b, *E*TRX_ox; c, *E*TRX_red.

doxin (Trx-S_2) and reduced protein. The N-terminal side of the cysteine residue (Cys32) is known to be solvent-exposed and to have higher reactivity and lower pK_a than the C-terminal side of cysteine (Cys35) in the active site (Figure 1). The low pK_a value is suggested to arise from the partial positive charge induced by a helix dipole from helix α2 (*61*). Also Asp26 and Lys57 ϵ-amino groups significantly affect the pK_a of the active-site thiol. The redox potential of protein is known to be dependent on the pK_a of the active-site thiol (*62*). The higher the pK_a of the active-site thiol, the lower the redox potential of the thioredoxin. In *Mj*TRX, cysteines in the active site are in the same secondary structural elements as in *E*TRX. The N-terminal side cysteine, Cys14, is in the loop between sheet β1 and helix α1, and the C-terminal side cysteine, Cys17, is in the α1 helix, which is similar to the active-site cysteines in *E*TRX. The tertiary interactions around this region are expected to be similar to those in *E*TRX, inferring from the T7 DNA polymerase interactions. However, pK_a values of both thiol groups in the active site are about 6.28. In *E*TRX, pK_a values of Cys32 and Cys35 are estimated to be about 7.1 and 7.9, respectively (*63*). The pK_a values of active-site cysteines are still controversial (*64*−*68*), but everyone agrees that Cys32 has a lower pK_a value than Cys35. In the case of *Mj*TRX, Cys14 would have a helix dipole effect, but the suggested residues (Asp26 and Lys57 in *E*TRX) influencing the pK_a value of the N-terminal side cysteine are not conserved. It is interesting that both thiol groups of *E. coli* D26A mutant thioredoxin have pK_a values of 7.5 (*69*). The conservation of a negatively charged residue at the position of Asp26 in *E*TRX appears to be related to the lower pK_a value of the N-terminal side of cysteine than the other cysteine. In DsbA, the N-terminal side of the cysteine, Cys30, has an abnormally low pK_a value of 3.42, and Glu24 is located at that position (*50*). The lack of a negatively charged residue at the Asp26 position in *Mj*TRX seems to be the reason for the simultaneous titration of the active-site cysteines. On the other hand, the low pK_a values of *Mj*TRX are related to the residues between two active cysteines. *Mj*TRX has Pro-His between two cysteines, which are the same residues found in DsbA. Substituting amino acid residues between two cysteines in DsbA changed the pK_a values of the cysteines. The pK_a value of Cys30 in DsbA was changed from 3.42 to 6.73 by changing the dipeptide from Pro-His to Pro-Pro (*50*). According to Szajewski and Whitesides (*70*), relative pK_a values of SH groups govern the reaction direction in the thiol exchange reaction. The group with the lower pK_a value becomes a better oxidizing catalyst. However, the pK_a value of *Mj*TRX is lower than that of *E*TRX although *Mj*TRX is a better reducing catalyst than *E*TRX. This implies that once a substrate binds to the protein, the pK_a value of the remaining thiol group could be changed, and the changed pK_a value affects the reactivity of the thiol group (*38*). The higher specific activity of *Mj*TRX in the insulin reduction is consistent with the lower redox potential of *Mj*TRX compared to that of *E*TRX. The standard state redox potential does not always predict the direction of the redox reaction, but the environment is another key factor. DsbA in the periplasm in *E. coli* could be replaced by the exported *E*TRX although the standard state redox potentials are very different (*72*). The redox potential of *Mj*TRX may also represent the environments microorganisms inhabit. The reduced redox potential of thioredoxin of *M. jannaschii* implies that this microorganism inhabits more reduced environments.

The redox potential of the *E. coli* cytosol has been estimated to be approximately −260 to −280 mV (*71*), and the thioredoxin and the glutathione/glutaredoxin systems play a critical role in maintaining the reducing environment (*49*). However, a single thioredoxin system has been found in *M. jannaschii* (*22*), and in the conserved neighbor, *Methanobacterium thermoautotrophicum* (*23*). It indicates that a single thioredoxin-like protein with the low redox potential, possibly with multiple functions conserved in glutaredoxin-like structure, is enough to maintain redox homeostasis in the archaeal methanogens.

REFERENCES

1. Holmgren, A. (1981) *Curr. Top Cell. Regul. 19*, 47−76.
2. Holmgren, A. (1985) *Annu. Rev. Biochem. 54*, 237−271.
3. Holmgren, A. (1989) *J. Biol. Chem. 264*, 13963−13966.
4. Lim, C. J., Haller, B., and Fuchs, J. A. (1985) *J. Bacteriol. 161*, 799−802.
5. Russel, M., and Model, P. (1986) *J. Biol. Chem. 261*, 14997−15005.
6. Feng, J. N., Russel, M., and Model, P. (1997) *Proc. Natl. Acad. Sci. U.S.A. 94*, 4068−4073.
7. Mark, D. F., and Richardson, C. C. (1976) *Proc. Natl. Acad. Sci. U.S.A. 73*, 780−784.
8. Adler, S., and Modrich, P. (1979) *J. Biol. Chem. 254*, 11605−11614.
9. Modrich, P., and Richardson, C. C. (1975) *J. Biol. Chem. 250*, 5508−5514.
10. Modrich, P., and Richardson, C. C. (1975) *J. Biol. Chem. 250*, 5515−5522.
11. Huber, H. E., Tabor, S., and Richardson, C. C. (1987) *J. Biol. Chem. 262*, 16224−16232.
12. Hoog, J. O., Jornvall, H., Holmgren, A., Carlquist, M., and Persson, M. (1983) *Eur. J. Biochem. 136*, 223−232.

13. Åslund, F., Ehn, B., Miranda-Vizuete, A., Pueyo, C., and Holmgren, A. (1994) *Proc. Natl. Acad. Sci. U.S.A. 91*, 9813−9817.
14. Martin, J. L. (1995) *Structure 3*, 245−250.
15. Bardwell, J. C., McGovern, K., and Beckwith, J. (1991) *Cell 67*, 581−589.
16. Darby, N. J., and Creighton, T. E. (1995) *Biochemistry 34*, 16770−16780.
17. Åslund, F., and Beckwith, J. (1999) *Cell 96*, 751−753.
18. Ding, H., and Demple, B. (1998) *Biochemistry 37*, 17280−17286.
19. Jakob, U., Muse, W., Eser, M., and Bardwell, J. C. (1999) *Cell 96*, 341−352.
20. Ruddock, L. W., and Klappa, P. (1999) *Curr. Biol. 9*, R400−402.
21. Zheng, M., Åslund, F., and Storz, G. (1998) *Science 279*, 1718−1721.
22. Bult, C. J., White, O., Olsen, G. J., Zhou, L., Fleischmann, R. D., Sutton, G. G., Blake, J. A., FitzGerald, L. M., Clayton, R. A., Gocayne, J. D., Kerlavage, A. R., Dougherty, B. A., Tomb, J. F., Adams, M. D., Reich, C. I., Overbeek, R., Kirkness, E. F., Weinstock, K. G., Merrick, J. M., Glodek, A., Scott, J. L., Geoghagen, N. S. M., and Venter, J. C. (1996) *Science 273*, 1058−1073.
23. Smith, D. R., Doucette-Stamm, L. A., Deloughery, C., Lee, H., Dubois, J., Aldredge, T., Bashirzadeh, R., Blakely, D., Cook, R., Gilbert, K., Harrison, D., Hoang, L., Keagle, P., Lumm, W., Pothier, B., Qiu, D., Spadafora, R., Vicaire, R., Wang, Y., Wierzbowski, J., Gibson, R., Jiwani, N., Caruso, A., Bush, D., and Reeve, J. N. (1997) *J. Bacteriol. 179*, 7135−7155.
24. Kawarabayasi, Y., Sawada, M., Horikawa, H., Haikawa, Y., Hino, Y., Yamamoto, S., Sekine, M., Baba, S., Kosugi, H., Hosoyama, A., Nagai, Y., Sakai, M., Ogura, K., Otsuka, R., Nakazawa, H., Takamiya, M., Ohfuku, Y., Funahashi, T., Tanaka, T., Kudoh, Y., Yamazaki, J., Kushida, N., Oguchi, A., Aoki, K., and Kikuchi, H. (1998) *DNA Res. 5*, 147−155.
25. Klenk, H. P., Clayton, R. A., Tomb, J. F., White, O., Nelson, K. E., Ketchum, K. A., Dodson, R. J., Gwinn, M., Hickey, E. K., Peterson, J. D., Richardson, D. L., Kerlavage, A. R., Graham, D. E., Kyrpides, N. C., Fleischmann, R. D., Quackenbush, J., Lee, N. H., Sutton, G. G., Gill, S., Kirkness, E. F., Dougherty, B. A., McKenney, K., Adams, M. D., Loftus, B., and Venter, J. C. (1997) *Nature 390*, 364−370.
26. Kawarabayasi, Y., Hino, Y., Horikawa, H., Yamazaki, S., Haikawa, Y., Jin-no, K., Takahashi, M., Sekine, M., Baba, S., Ankai, A., Kosugi, H., Hosoyama, A., Fukui, S., Nagai, Y., Nishijima, K., Nakazawa, H., Takamiya, M., Masuda, S., Funahashi, T., Tanaka, T., Kudoh, Y., Yamazaki, J., Kushida, N., Oguchi, A., and Kikuchi, H. (1999) *DNA Res. 6*, 83−101, 145−152.
27. Deckert, G., Warren, P. V., Gaasterland, T., Young, W. G., Lenox, A. L., Graham, D. E., Overbeek, R., Snead, M. A., Keller, M., Aujay, M., Huber, R., Feldman, R. A., Short, J. M., Olsen, G. J., and Swanson, R. V. (1998) *Nature 392*, 353−358.
28. Nelson, K. E., Clayton, R. A., Gill, S. R., Gwinn, M. L., Dodson, R. J., Haft, D. H., Hickey, E. K., Peterson, J. D., Nelson, W. C., Ketchum, K. A., McDonald, L., Utterback, T. R., Malek, J. A., Linher, K. D., Garrett, M. M., Stewart, A. M., Cotton, M. D., Pratt, M. S., Phillips, C. A., Richardson, D., Heidelberg, J., Sutton, G. G., Fleischmann, R. D., Eisen, J. A., and Fraser, C. M. (1999) *Nature 399*, 323−329.
29. Baross, J. A., and Holden, J. F. (1996) *Adv. Protein Chem. 48*, 1−34.
30. Adams, M. W. (1993) *Annu. Rev. Microbiol. 47*, 627−658.
31. Guagliardi, A., de Pascale, D., Cannio, R., Nobile, V., Bartolucci, S., and Rossi, M. (1995) *J. Biol. Chem. 270*, 5748−5755.
32. Langsetmo, K., Fuchs, J., and Woodward, C. (1989) *Biochemistry 28*, 3211−3220.
33. Holmgren, A. (1979) *J. Biol. Chem. 254*, 9627−9632.
34. Holmgren, A. (1979) *J. Biol. Chem. 254*, 9113−9119.
35. Gan, Z. R., and Wells, W. W. (1986) *J. Biol. Chem. 261*, 996−1001.
36. Pace, C. N., Vajdos, F., Fee, L., Grimsley, G., and Gray, T. (1995) *Protein Sci. 4*, 2411−2423.
37. Polgar, L. (1974) *FEBS Lett. 47*, 15−18.
38. Graminski, G. F., Kubo, Y., and Armstrong, R. N. (1989) *Biochemistry 28*, 3562−3568.
39. Nelson, J. W., and Creighton, T. E. (1994) *Biochemistry 33*, 5974−5983.
40. Huber, H. E., Russel, M., Model, P., and Richardson, C. C. (1986) *J. Biol. Chem. 261*, 15006−15012.
41. Zhang, O., Kay, L. E., Olivier, J. P., and Forman-Kay, J. D. (1994) *J. Biomol. NMR 4*, 845−858.
42. Kuboniwa, H., Grzesiek, S., Delaglio, F., and Bax, A. (1994) *J. Biomol. NMR 4*, 871−878.
43. Grzesiek, S., and Bax, A. (1993) *J. Magn. Reson. B 101*, 114−119.
44. Ikura, M., Kay, L. E., and Bax, A. (1990) *Biochemistry 29*, 4659−4667.
45. Pascal, S. M., Singer, A. U., Gish, G., Yamazaki, T., Shoelson, S. E., Pawson, T., Kay, L. E., and Forman-Kay, J. D. (1994) *Cell 77*, 461−472.
46. Muhandiram, D. R., and Kay, L. E. (1994) *J. Magn. Reson. B 103*, 203−216.
47. Delaglio, F., Grzesiek, S., Vuister, G. W., Zhu, G., Pfeifer, J., and Bax, A. (1995) *J. Biomol. NMR 6*, 277−293.
48. Wishart, D. S., and Sykes, B. D. (1994) *J. Biomol. NMR 4*, 171−180.
49. Åslund, F., Berndt, K. D., and Holmgren, A. (1997) *J. Biol. Chem. 272*, 30780−30786.
50. Grauschopf, U., Winther, J. R., Korber, P., Zander, T., Dallinger, P., and Bardwell, J. C. (1995) *Cell 83*, 947−955.
51. Wüthrich, K. (1986) *NMR of Proteins and Nucleic Acids*, John Wiley and Sons, New York.
52. Lim, C. J., Gleason, F. K., and Fuchs, J. A. (1986) *J. Bacteriol. 168*, 1258−1264.
53. Powles, R. E., Deane, S. M., and Rawlings, D. E. (1995) *Microbiology 141*, 2175−2181.
54. Lim, C. J., Sa, J. H., and Fuchs, J. A. (1996) *Biochim. Biophys. Acta 1307*, 13−16.
55. Pille, S., Assemat, K., Breton, A. M., and Clement-Metral, J. D. (1996) *Eur. J. Biochem. 235*, 713−720.
56. Doublie, S., Tabor, S., Long, A. M., Richardson, C. C., and Ellenberger, T. (1998) *Nature 391*, 251−258.
57. Dyson, H. J., Jeng, M. F., Model, P., and Holmgren, A. (1994) *FEBS Lett. 339*, 11−17.
58. Wunderlich, M., and Glockshuber, R. (1993) *Protein Sci. 2*, 717−726.
59. Chivers, P. T., Laboissiere, M. C., and Raines, R. T. (1996) *EMBO J. 15*, 2659−2667.
60. Rossmann, R., Stern, D., Loferer, H., Jacobi, A., Glockshuber, R., and Hennecke, H. (1997) *FEBS Lett. 406*, 249−254.
61. Holmgren, A. (1995) *Structure 3*, 239−243.
62. Warwicker, J. (1998) *J. Biol. Chem. 273*, 2501−2504.
63. Li, H., Hanson, C., Fuchs, J. A., Woodward, C., and Thomas, G. J., Jr. (1993) *Biochemistry 32*, 5800−5808.
64. Wilson, N. A., Barbar, E., Fuchs, J. A., and Woodward, C. (1995) *Biochemistry 34*, 8931−8939.
65. Jeng, M. F., and Dyson, H. J. (1996) *Biochemistry 35*, 1−6.
66. LeMaster, D. M. (1996) *Biochemistry 35*, 14876−14881.
67. Takahashi, N., and Creighton, T. E. (1996) *Biochemistry 35*, 8342−8353.
68. Dyson, H. J., Jeng, M. F., Tennant, L. L., Slaby, I., Lindell, M., Cui, D. S., Kuprin, S., and Holmgren, A. (1997) *Biochemistry 36*, 2622−2636.
69. Vohnik, S., Hanson, C., Tuma, R., Fuchs, J. A., Woodward, C., and Thomas, G. J., Jr. (1998) *Protein Sci. 7*, 193−200.
70. Szajewski, R. P., and Whitesides, G. M. (1980) *J. Am. Chem. Soc. 102*, 2011−2026.
71. Hwang, C., Sinskey, A. J., and Lodish, H. F. (1992) *Science 257*, 1496−1502.
72. Debarbieux, L., and Beckwith, J. (2000) *J. Bacteriol. 182*, 723−727.

BI000035B